

ATTAR, S., CHEN, B., CATALANOTTI, G. and FALZON, B.G. 2023. Tensile and impact properties of melt-blended nylon 6/ethylene-octene copolymer/graphene oxide nanocomposites. In *Falzon, B.G. and McCarthy, C. (eds.) Proceedings of the 23rd International conference on composite materials 2023 (ICCM 23), 30 July - 04 August 2023, Belfast, Northern Ireland*. Belfast: Queen's University Belfast. Hosted on ICCM-central [online], paper 253. Available from: <http://www.iccm-central.org/Proceedings/ICCM23proceedings/index.htm>

# Tensile and impact properties of melt-blended nylon 6/ethylene-octene copolymer/graphene oxide nanocomposites.

ATTAR, S., CHEN, B., CATALANOTTI, G. and FALZON, B.G.

2023

## TENSILE AND IMPACT PROPERTIES OF MELT-BLENDED NYLON 6/ETHYLENE-OCTENE COPOLYMER/GRAPHENE OXIDE NANOCOMPOSITES

Suhail Attar<sup>1\*</sup>, Biqiong Chen<sup>2</sup>, Giuseppe Catalanotti<sup>3</sup> and Brian G. Falzon<sup>4</sup>

<sup>1</sup> School of Engineering, Robert Gordon University, Aberdeen, AB10 7GJ, United Kingdom

<sup>2</sup> School of Mechanical and Aerospace Engineering, Queen's University Belfast, BT9 5AH, United Kingdom

<sup>3</sup> Department of Mechatronics Engineering, University of Évora, Rua do Cardeal Rei, s/n, 7000-849 Évora Largo dos Colegiais, N° 2, 7004-516 Évora, Portugal

<sup>4</sup> School of Engineering, STEM College, RMIT University, GPO Box 2476, Melbourne, 3001, Victoria, Australia

\* Corresponding author (s.attar@rgu.ac.uk)

**Keywords:** Nylon 6, Graphene oxide, Mechanical properties

### ABSTRACT

The addition of stiff nanoparticles to a polymer matrix usually proves beneficial for the enhancement in stiffness and strength, however, the impact strength is usually lowered. Conversely, the use of elastomeric additives can enhance the toughness and impact strength but causes a reduction in overall stiffness and strength. To take advantage of the desirable effects of both additives, they may be simultaneously added to the host matrix. Graphene oxide (GO), along with a thermoplastic elastomer ethylene-octene copolymer (EOC), was chosen to be added to nylon 6 for the current investigation. Maleated EOC (EOC-g-MA) was used as a compatibilizer for this study. 3 wt% GO nanoparticles, 20 wt% ethylene-octene copolymer (EOC) and 3 wt% EOC-g-MA were added to nylon 6 to prepare the nylon 6/EOC/GO blend-based nanocomposites. A high shear rate screw running at 300 rpm was used for melt-blending with a twin-screw extruder.

Increased stiffness and tensile strength were observed by the addition of GO nanoparticles while elongation at break, toughness and impact strength were lowered by the addition of GO. The addition of EOC and EOC-g-MA enhanced the elongation at break, toughness and impact strength. However, the stiffness and strength of nylon 6/EOC blend was lower than that of the neat nylon 6. The addition of GO nanoparticles and EOC to neat nylon 6 caused a reduction in its impact strength. However, simultaneous addition of EOC and EOC-g-MA to nylon 6 caused a significant increase in the impact strength compared to neat nylon 6 and yielded a nylon 6/EOC/EOC-g-MA blend with the highest impact strength. The addition of GO nanoparticles to this blend, however, again caused a significant reduction in the impact strength. Nylon 6/ EOC/EOC-g-MA blend showed the highest toughness and impact strength. Simultaneous addition of EOC and GO helped achieve a balanced stiffness and toughness.

### 1 INTRODUCTION

Mechanical properties of polymer nanocomposites depend on several variables like intrinsic properties of polymer matrix and nano particles, their interfacial interaction and dispersion of nanoparticles in the polymer matrix [1]–[3]. Interfacial interaction between the two constituents depends on the presence of functional groups which also facilitates the dispersion of nanoparticles. Enhanced dispersion increases the interfacial area between the two constituents and causes a reduction in the size of agglomerates [4]–[6]. Several investigations have been carried out to study the influence of graphene and graphene-based nanoparticles on the mechanical properties of different polymer matrices [7]–[13].

Based on the experimental results it is believed that the addition of functionalized graphene can toughen the polymers, however the understanding of the mechanism is still insufficient [14].

Jin et al. [13] prepared and characterized nanocomposites based on nylon 11 and 12 using functionalized graphene (FG). In the case of nylon 12, the ultimate tensile strength increased by 35%, fracture toughness by 75% and the impact failure energy by 85%, respectively. A dramatic enhancement of 250% in impact strength was achieved by adding 1 wt% FG to nylon 11. Similarly, nylon 11/GO nanocomposites prepared by Yuan et al. [15] showed enhanced stiffness and toughness. The impact strength of the composite increased by 52% as compared with neat nylon 11. In another attempt by Neill et al. [16] nylon 6/graphene nanocomposites were prepared with single layer GO and chemically reduced GO (rGO). An enhancement in the thermal stability and crystallinity of the developed nanocomposites was observed. Graphene oxide showed better interfacial interaction with the polymer compared to rGO due to the functionalization of GO.

An investigation by Pramoda [17] investigated the influence of addition of functionalized graphene on the mechanical and thermal properties of resultant nanocomposites. The glass transition temperature ( $T_g$ ) was increased by 31% and 55% for two nanocomposites. This study showed that an increase in the thermomechanical properties of nanocomposites can be achieved by developing a strong interface between the two constituents. Shang et al. [8] carried out an investigation to study the effect of folded or crumpled GnP morphology on the mechanical properties of polymer nanocomposites. Attempts for toughening other thermoplastic polymers like polyurethane, low density polyethylene and polyvinyl alcohol by using functionalized graphene have also been done [18]–[20]. Toughening of epoxy using graphene and its derivatives was done by Tang et al. [21] and other researchers [11], [22], [23].

Pristine nanoparticles exhibit a weak interaction with the host polymer therefore graphene oxide was chosen for this study which was expected to have a stronger interaction with nylon 6. Such strong interfacial interaction might improve the mechanical properties of resultant nanocomposites. Tensile strength of polymer nanocomposites has been observed to improve due to strong interfacial interactions [10], [24]. Graphene oxide may result in the brittleness of resultant nanocomposites which requires addition of an elastomeric phase. EOC was therefore chosen for the preparation of nylon 6/EOC blend-based nanocomposites. EOC-g-MA was used to enhance the interaction between the two ingredients. A loading level of 20 wt% EOC was used based on the literature survey [25], [26] which showed that brittle-ductile transition was achieved at about 20 wt% loading level. A loading level of 3 wt% was chosen for EOC-g-MA since a higher wt% of maleic anhydride was considered detrimental to the properties of the blend as documented in the literature [27], [28], [29].

## 2 EXPERIMENTAL

### 2.1 Materials

Nylon 6 grade Akulon<sup>®</sup> F223-D, a product of DSM Engineering Plastics purchased from Resinex UK, was used in the current work. Graphene oxide nanoparticles (ECO GO Grade A) as multilayer stacks (1-4 layers) of graphene sheets were supplied by Graphitene UK. Ethylene-octene copolymer (EOC, grade Engage 8150) was also obtained from Resinex UK which is a product of DuPont Dow elastomers. Maleated EOC (grade Fusabond 463) EOC-g-MA was kindly provided by DuPont Dow elastomers.

### 2.2 Preparation of nylon 6 nanocomposites and their test samples

Nylon 6 pellets were cooled to very low temperatures using liquid nitrogen and ground into powder form using a Wedco SE-12 UR pilot plant grinding mill at 7000 rpm and a gap size 400  $\mu\text{m}$ . The powder was examined using a stereo microscope (Nikon SMZ800) and the particle size distribution was found to be 100-300  $\mu\text{m}$ . The powder was dried overnight at 80  $^{\circ}\text{C}$  using a dryer (Carbolite). Pre-mixing of Nylon 6 with 3 wt% of GO, 20 wt% EOC and 3 wt% EOC-g-MA was done using a Thermo Scientific Prism Pilot 3 High Speed Mixer at 3000 rpm for 4 minutes. Melt blending of nanocomposites was

performed using high shear screw design at 300 rpm. Temperature of the barrel of twin-screw extruder for melt blending operation for zone 1-3 was 260 °C, zone 4-5 was 270 °C and die was at 260 °C.

The extruded nanocomposite and neat nylon 6 pellets were ground into fine powder for compression moulding using a Rondol freezer mill. Pellets were ground for 10 cycles each of 2 minutes with a cooling interval of 2.5 minutes. A pre-cool time of 10 minutes and an impacting frequency of 15 Hz was used for grinding. Particle size analysis was performed using a stereo microscope and particle size was found to be around 100 µm. The powder was dried overnight at 80 °C prior to compression moulding using in-house made moulds. Moulds were filled with dried powder and placed in a platen press (Collin PCS II). The platen press was then closed, and a pre-programmed cycle of time and temperature was started. Processing conditions used for compression moulding of specimens are detailed in Table 1. Tensile test specimens, according to the BS ISO 527 (Type 1BA) standard, were prepared by injection moulding using a Rondol high force 5 small injection moulding machine.

<b>Phase</b>	<b>1</b>	<b>2</b>	<b>3</b>	<b>4</b>	<b>5</b>
<b>Upper platen temperature (°C)</b>	245	250	250	150	80
<b>Lower platen temperature (°C)</b>	245	250	250	150	80
<b>Pressure (Bar)</b>	9	13	17	17	17
<b>Time (Sec)</b>	600	800	240	180	180

Table 1: Processing conditions used for compression moulding

### 2.3 Characterisation of nylon 6 nanocomposites

Fourier Transform Infrared Spectroscopy (FTIR) was carried out using a Perkin Elmer Spectrum 100 spectrometer with an ATR sampling accessory. All the spectra were recorded at a resolution of 4 cm<sup>-1</sup> with an accumulation of 32 scans in mid infrared region of 4000-650 cm<sup>-1</sup>.

Differential scanning calorimetry (DSC) was carried out using Perkin Elmer DSC model 6 under an inert nitrogen environment. A heating and cooling rate of 10 °C/min was used to heat the samples between 30 °C and 250 °C. In all cases the samples were held at 250 °C for 2 mins, then cooled to 30 °C at 10 °C/min and reheated to 250 °C at 10 °C/min. Second heating scan was run to remove the thermal history.

Tensile tests were conducted according to BS ISO 527 using a Zwick Tester with a 10 kN load cell and a crosshead speed of 5 mm/min. Five specimens were tested for each sample. For elastic modulus measurements, nominal strain (up to the yield point) was determined using an extensometer attached to the gauge section of the tensile specimens.

Charpy impact tests were conducted using a Resil impact tester with a 7.5 J hammer, according to BS ISO 179, at room temperature. Ten specimens were tested for neat nylon 6 and nanocomposite samples.

Dynamic Mechanical Analysis (DMA) was performed using a Perkin Elmer DMA 8000 in single cantilever bending mode with beam length of 20 mm and loading frequency of 1 Hz. A temperature scan from 30 °C to 110 °C was run at a temperature ramp of 2 °C/min.

### 3 RESULTS AND DISCUSSION

#### 3.1 Structure

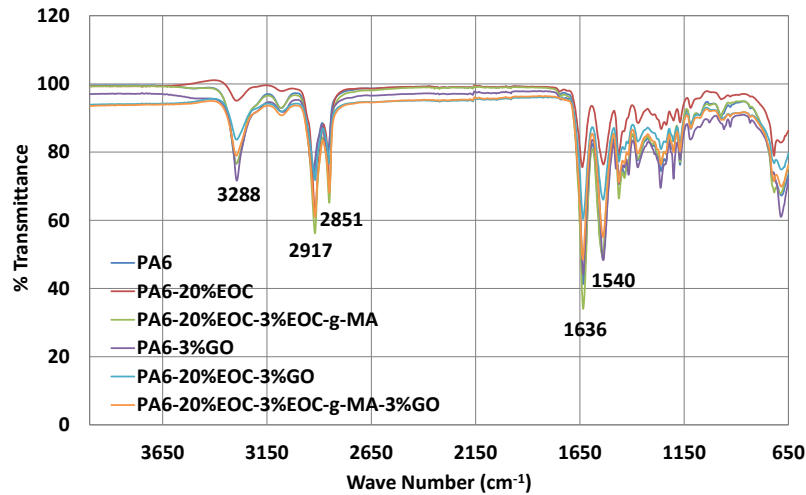


Figure 1: FTIR spectra of nylon 6, nylon 6/EOC blend and blend-based nanocomposites

FTIR scans of nylon 6, nylon 6/EOC blends and nanocomposites, shown in Figure 1, were performed to see any possible interactions between different constituents. Most of the typical absorption bands of neat nylon 6 remained unchanged even after addition of GO, EOC or EOC-g-MA and no new absorption band was observed. A stretching vibration of the N-H amide linkage was observed at  $3297\text{ cm}^{-1}$  and stretching vibrations of the amide-I and amide-II were observed at  $1641\text{ cm}^{-1}$  and  $1542\text{ cm}^{-1}$ . Peaks observed at  $2868\text{ cm}^{-1}$  and  $2938\text{ cm}^{-1}$  are characterized as stretching vibrations of aliphatic C-H bonds. The reaction of maleic anhydride group on the compatibilizer and amine group on nylon 6 might have formed functional groups of C=O and NH [30]. Absorption peaks of these groups overlap the original absorption regions, so they are not clearly discernible [31].

DSC was performed to investigate any influence of the addition of EOC and GO on the melting and crystallization of nylon 6. Second heating and cooling DSC curves are shown in Figure 2. Melting temperature, enthalpy of fusion, % crystallinity and crystallization temperature are tabulated in Table 2.

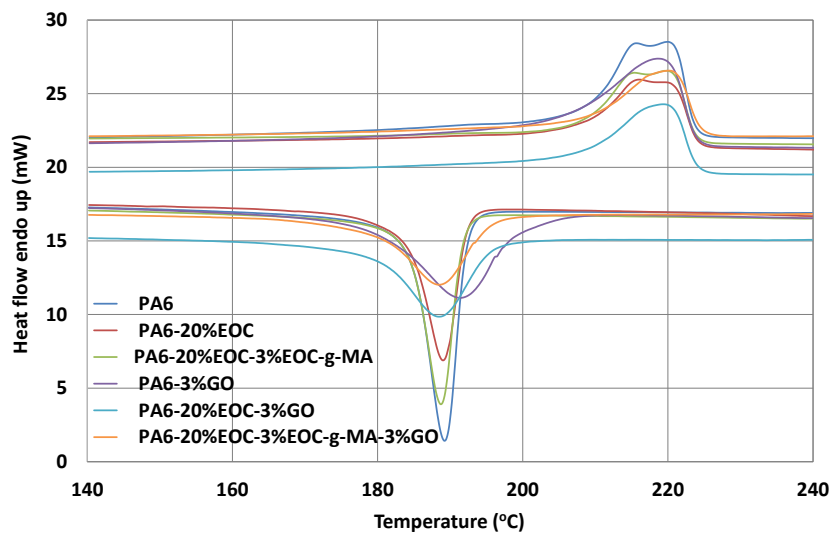


Figure 2: Cooling and 2<sup>nd</sup> DSC heating curve for nylon 6, nylon 6/EOC blends and nanocomposites

Sample ID	2nd Heating			Cooling
	Melting temp $T_m$ (°C)	Enthalpy of fusion $\Delta H$ (J/g)	% Crystallinity $X_c$ (%)	Crystallization temp $T_c$ (°C)
PA6	220.0	53.5	28.5	189.2
PA6-20%EOC	216.3	38.4	25.5	189.0
PA6-20%EOC-3%EOC-g-MA	219.8	42.8	29.6	188.6
PA6-3%GO	218.6	65.5	35.9	191.3
PA6-20%EOC-3%GO	219.5	39.2	27.1	188.4
PA6-20%EOC-3%EOC-g-MA-3%GO	220.1	34.7	24.9	188.4

Table 2: DSC results for nylon 6, nylon 6/EOC and nylon 6/EOC/GO nanocomposites

The second heating curve of neat nylon 6 showed two peaks, a lower one at 214 °C for  $\gamma$ - crystallites and a higher peak at 220 °C for  $\alpha$ -form crystals [32], [33]. Addition of EOC to neat nylon 6 had little or no effect on the two melting peaks. Addition of the compatibilizer EOC-g-MA to nylon 6/EOC blend again showed a heating curve with two melting peaks at 214 °C and 220 °C. By addition of GO nanoparticles in neat nylon 6, the lower melting peak disappeared, leaving only the melting of the  $\alpha$ -form crystallites. This could be due to the stabilizing effect of GO nanoparticles on the crystallization phenomenon. Both nylon 6/EOC/GO nanocomposites and nylon 6/EOC/EOC-g-MA/GO nanocomposites exhibited a single melting peak at about 220 °C.

The crystallinity of neat nylon 6 was estimated to be 28.5% while a % crystallinity of 25.5% was observed for nylon 6/EOC blend. This reduction in % crystallinity is a possible outcome of the hindrance offered by EOC to nylon 6 chains to form crystals. Addition of the compatibilizer caused a slight increase in % crystallinity of the nylon 6/EOC blend. A higher % crystallinity, 35.9%, was observed for nylon 6/GO nanocomposites which is likely due to GO nanoparticles acting as the nucleation sites for crystallization [34]. A % crystallinity of 27.1% for nylon 6/EOC/GO nanocomposites was slightly higher than the corresponding nylon 6/EOC blend while a degree of crystallinity of 24.9% for nylon 6/EOC/EOC-g-MA/GO nanocomposite was lower than that for the corresponding blend.

### 3.2 Mechanical properties

Tensile tests were carried out to measure the tensile properties. Representative tensile test curves of neat nylon 6, nylon 6/EOC blends and blend-based nanocomposites are shown in Figure 3 and measured values are tabulated in Table 3.

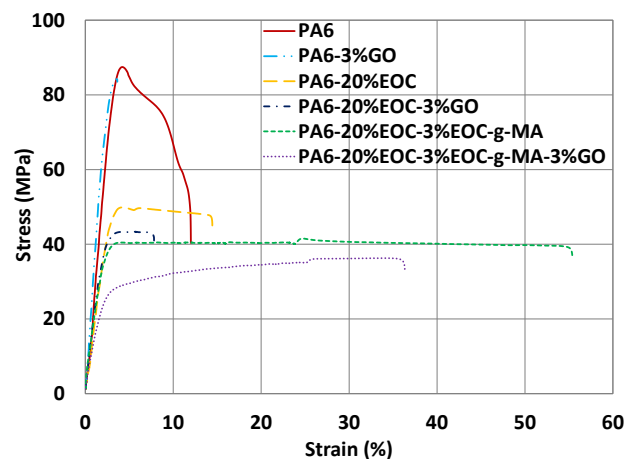


Figure 3: Tensile stress-strain curves for nylon 6, nylon 6/EOC blends and nanocomposites

Materials	Young's modulus (GPa)	SD	Tensile strength (MPa)	SD	Strain at break (%)	SD	Toughness (J/m <sup>3</sup> )	SD
<b>PA6</b>	2.8	0.2	87.0	0.5	11.8	0.6	806.9	34.8
<b>PA6-20%E0C</b>	1.8	0.1	50.3	0.5	14.8	0.4	678.5	25.0
<b>PA6-20%E0C-3%E0C-g-MA</b>	1.5	0.1	40.2	0.2	54.6	1.8	2160.7	72.8
<b>PA6-3%GO</b>	3.4	0.2	84.9	0.9	3.5	0.2	199.8	21.3
<b>PA6-20%E0C-3%GO</b>	1.8	0.0	42.4	0.3	7.4	0.3	298.5	4.7
<b>PA6-20%E0C-3%E0C-g-MA-3%GO</b>	1.3	0.0	36.6	0.2	36.4	0.2	1211.6	14.8

Table 3: Tensile test results of nylon 6/E0C/GO nanocomposites

Neat nylon 6 exhibited a Young's modulus of  $2.8 \pm 0.2$  GPa while nylon 6/GO nanocomposites showed a tensile modulus of  $3.4 \pm 0.2$  GPa, which was an outcome of much higher Young's modulus ( $\sim 207$  GPa) [35] of GO nanoparticles. Also GO nanoparticles may have generated a strong interface causing an increase in the overall stiffness of nanocomposites. Nylon 6 and nylon 6/GO nanocomposites exhibited similar tensile strengths of  $87.0 \pm 0.5$  MPa and  $85.0 \pm 0.9$  MPa respectively while all other samples showed a lower tensile strength. Tensile strength of nanocomposites has been found to strongly depend upon interfacial strength [3]. A reduced strain at break of 3.5% was observed for nylon 6/GO nanocomposites due to constrained polymer chain movement [1], [3], [16]. Degradation of nylon 6 due to oxidation with GO might have also contributed towards lower strain at break of nanocomposites. Correspondingly, nylon 6 exhibited a higher toughness of  $806.9 \pm 34.8$  J/m<sup>3</sup> while nylon 6/GO nanocomposites had a toughness of  $199.8 \pm 21.3$  J/m<sup>3</sup>.

A reduced stiffness and tensile strength was observed for nylon 6/E0C blend as compared to neat nylon 6, which could be due to the elastomeric nature, lower tensile strength and poor compatibility of E0C with nylon 6. An increase in the strain at break for nylon 6/E0C blend was observed due to elastomeric nature of E0C, however due to low miscibility, the influence of E0C was not that pronounced. A reduction in the toughness of nylon 6/E0C blend was observed compared to neat nylon 6 despite a minor increase in strain at break. E0C lowered the stiffness and toughness of nylon 6.

Addition of E0C-g-MA to nylon 6/E0C blend caused a further reduction in the stiffness and tensile strength of the blend which showed a Young's modulus of  $1.5 \pm 0.1$  GPa and tensile strength of  $40.2 \pm 0.2$  MPa. Enhanced compatibility between E0C and nylon 6 caused a more pronounced effect of E0C on nylon 6 and hence a reduction in the strength and stiffness [28]. However, a significant increase in the strain at break of compatibilized nylon 6/E0C blend was observed which showed a strain at break of  $54.6 \pm 1.8\%$ . Compatibilized nylon 6/E0C blend showed a toughness of  $2160.7 \pm 72.8$  J/m<sup>3</sup>.

Nylon 6/E0C/GO nanocomposites exhibited a Young's modulus of  $1.8 \pm 0.0$  GPa and a tensile strength of  $42.4 \pm 0.3$  MPa. Addition of GO to nylon 6/E0C blend slightly lowered the tensile strength of this blend while Young's modulus remained unaffected. A strain at break of  $7.4 \pm 0.3\%$  and a toughness value of  $298.5 \pm 4.7$  J/m<sup>3</sup> was observed for nylon 6/E0C/GO nanocomposites. A reduction in strain at break and toughness of nylon 6/E0C/GO nanocomposites can be attributed to the stiff nature of GO nanoparticles. Addition of GO to compatibilized nylon 6/E0C blend yielded a Young's modulus of  $1.3 \pm 0.0$  GPa and a tensile strength of  $36.6 \pm 0.2$  MPa while an elongation at break of  $36.4 \pm 0.2\%$  and toughness of  $1211.6 \pm 14.8$  J/m<sup>3</sup> was observed for this formulation. A reduction in the stiffness and strength of compatibilized nylon 6/E0C blend occurred by the addition of GO nanoparticles. Similarly, a higher reduction in the strain at break and toughness was observed for compatibilized blend-based

nanocomposites compared to their corresponding blend, possibly due to the constraining effect of GO on polymer chains.

Charpy impact tests of neat nylon 6, nylon 6/EOC blends and blend-based nanocomposites were conducted to study the influence of addition of EOC and GO on the impact strength of nylon 6. Impact strength of nylon 6 and nylon 6 blend-based nanocomposites is shown in Figure 4.

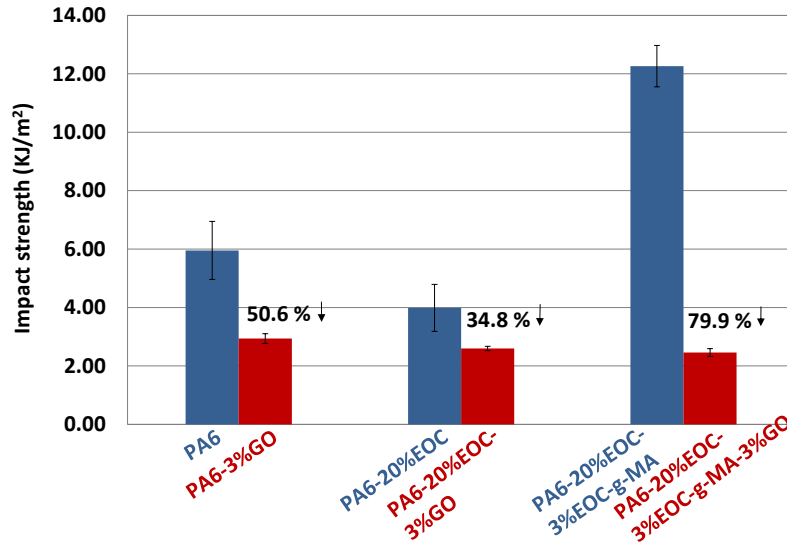


Figure 4: Impact strength of nylon 6, nylon 6/EOC blend and blend-based nanocomposites

Neat nylon 6 exhibited an impact strength of  $5.9 \pm 1.0$  kJ/m<sup>2</sup> which was reduced to  $2.9 \pm 0.2$  kJ/m<sup>2</sup> upon addition of GO nanoparticles. A reduction in the impact strength in this case could be due to stiff nature of GO nanoparticles. Also, formation of a constrained polymer chains' region and oxidation of nylon 6 by GO might contributed towards the reduction in the impact strength.

Addition of 20 wt% EOC to nylon 6 provided the blend with an impact strength of  $3.9 \pm 0.8$  kJ/m<sup>2</sup>. A reduction in the impact strength by addition of EOC was an outcome of the weak interfacial interaction between nylon 6 and EOC. Nylon 6/EOC/EOC-g-MA blend exhibited an impact strength of  $12.2 \pm 0.7$  kJ/m<sup>2</sup> which was higher than the impact strength of neat nylon 6 and nylon 6/EOC blend. This enhancement in impact strength was an outcome of the compatibilization effect of maleic anhydride group which gives a strong interface between nylon 6 and EOC.

Addition of 3 wt% GO to nylon 6/EOC blend caused a reduction in the impact strength of nylon 6/EOC blend which exhibited an impact strength of  $2.6 \pm 0.0$  kJ/m<sup>2</sup>. Simultaneous addition of EOC and GO to nylon 6 during melt blending might have caused some GO to go inside the dispersed EOC phase, which might have lowered the toughening capability of EOC. Similarly, addition of 3 wt% GO to compatibilized nylon 6/EOC blend also caused reduction in the impact strength where the compatibilized blend-based nanocomposite showed an impact strength value of  $2.4 \pm 0.1$  kJ/m<sup>2</sup>.

Dynamic mechanical analysis of nylon 6 and nylon 6 blend-based nanocomposites was done to study the effect of addition of EOC and GO on nylon 6. Figure 5 (a-c) shows the storage modulus, loss modulus and loss factor curves of nylon 6, nylon 6/EOC blend and blend-based nanocomposites.

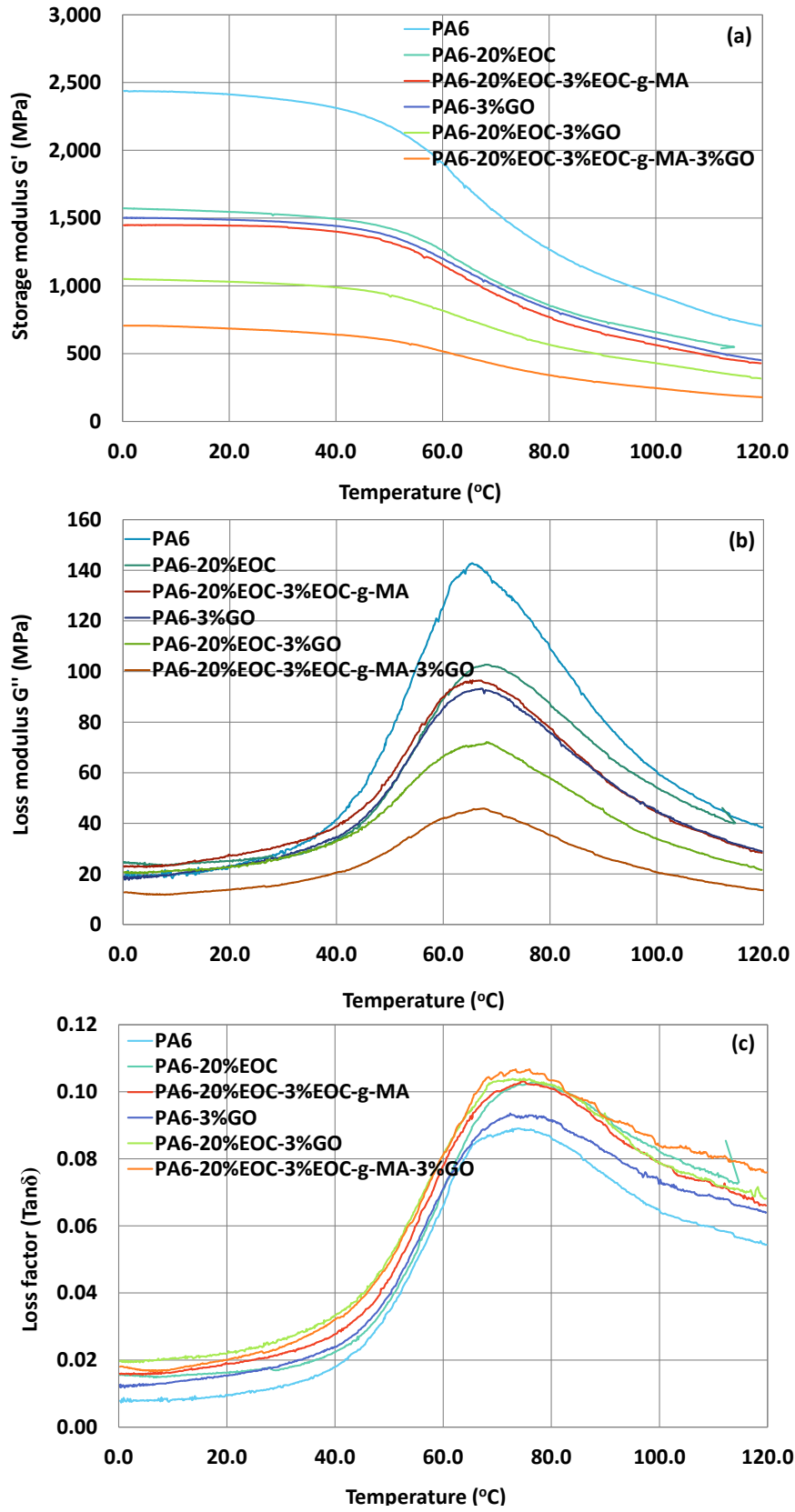


Figure 5: (a) Storage modulus, (b) loss modulus and (c) loss factor ( $\tan \delta$ ) curves of nylon 6, nylon 6/EOC blends and blend-based nanocomposites

Sample	Glass transition temperature $T_g$ (°C)
PA6	73.7
PA6-20%EOC	76.6
PA6-20%EOC-3%EOC-g-MA	74.6
PA6-3%GO	72.3
PA6-20%EOC-3%GO	73.0
PA6-20%EOC-3%EOC-g-MA-3%GO	75.4

Table 4: Glass transition temperature  $T_g$  of nylon 6 and nylon 6/EOC/GO nanocomposites

Storage moduli of nylon 6, nylon 6/EOC blends and blend-based nanocomposites is shown in Figure 5 (a). Neat nylon 6 exhibited the highest storage modulus over the whole temperature range tested while all the blends and blend-based nanocomposites showed lower storage modulus. Addition of GO to neat nylon 6 caused a reduction in the storage modulus which was more evident at lower temperatures and less evident at higher temperatures i.e. after glass transition. Also, it was observed that the storage modulus of nylon 6 was appreciably reduced by the addition of EOC over the whole temperature range. Addition of EOC-g-MA to the blend caused a further reduction in the storage modulus. It was observed that GO based nanocomposites and nylon 6/EOC blends exhibited nearly similar storage modulus values and trend of variation. A similar trend of reduction in the loss modulus of nylon 6/EOC blends and blend-based nanocomposites was observed as shown in Figure 5 (b). Addition of EOC and EOC-g-MA to nylon 6 caused a reduction in the loss modulus which was further lowered by the addition of GO nanoparticles. Loss modulus of nylon 6 and all other samples was nearly same at temperatures below than 40 °C, however, the reduction of loss modulus became prominent at higher temperature. Glass transition temperature was measured as the peak of  $\tan\delta$  curves shown in Figure 5 (c). Table 4 shows  $T_g$  of all the samples measured as peak of loss factor curve. The glass transition temperature of nylon 6/EOC blends and blend-based nanocomposites remained almost constant at around 75 °C. There was a minor effect of the addition of EOC and GO nanoparticles on polymer chain dynamics.

#### 4 CONCLUSIONS

It can be postulated that stiffness of the nanocomposites depends on the intrinsic stiffness of the additives apart, from other variables like loading level and dispersion. High tensile strength of nylon 6/GO nanocomposites is a likely outcome of the better interfacial interactions between nylon 6 and GO. Functionalized GO nanoparticles have a detrimental effect on the elongation at break and ductility. A reduction in the tensile strength of nylon 6 by the addition of EOC can be attributed to the elastic nature of EC and weak interface between the two. Stiff GO nanoparticles lowered the elongation at break and toughness while EOC had a positive influence on these two parameters. Impact strength was also observed to be opposingly influenced by these two additives. These observations indicate a balanced combination of tensile properties can be achieved by simultaneously adding the two types of additives. The loading level of nanoparticles and morphology of the nanocomposites also have a bearing on the resultant properties which must be controlled to get desired mechanical properties. This study shows the potential of improving the mechanical properties of nanocomposites by achieving a synergistic influence of the two types of additives.

#### ACKNOWLEDGEMENTS

I gratefully acknowledge the financial support of the project ICONIC — Improving the Crashworthiness of Composite Transportation Structures. ICONIC has received funding from the European Union's Horizon 2020 research and innovation programme under the Marie Skłodowska-Curie grant agreement No 721256. The content in this paper reflects only the researcher view and the Agency is not responsible for any use that may be made of the information it contains.

## REFERENCES

- [1] D. G. Papageorgiou, I. A. Kinloch, and R. J. Young, "Mechanical properties of graphene and graphene-based nanocomposites," *Prog. Mater. Sci.*, vol. 90, pp. 75–127, 2017, doi: 10.1016/j.pmatsci.2017.07.004.
- [2] K. Hu, D. D. Kulkarni, I. Choi, and V. V. Tsukruk, "Graphene-polymer nanocomposites for structural and functional applications," *Prog. Polym. Sci.*, vol. 39, no. 11, pp. 1934–1972, 2014, doi: 10.1016/j.progpolymsci.2014.03.001.
- [3] J. R. Potts, D. R. Dreyer, C. W. Bielawski, and R. S. Ruoff, "Graphene-based polymer nanocomposites," *Polymer (Guildf)*, vol. 52, no. 1, pp. 5–25, 2011, doi: 10.1016/j.polymer.2010.11.042.
- [4] H. Liu and L. C. Brinson, "Reinforcing efficiency of nanoparticles: A simple comparison for polymer nanocomposites," *Compos. Sci. Technol.*, vol. 68, no. 6, pp. 1502–1512, 2008, doi: 10.1016/j.compscitech.2007.10.033.
- [5] S. Pavlidou and C. D. Papaspyrides, "A review on polymer-layered silicate nanocomposites," *Prog. Polym. Sci.*, vol. 33, no. 12, pp. 1119–1198, 2008, doi: 10.1016/j.progpolymsci.2008.07.008.
- [6] S. Y. Fu, X. Q. Feng, B. Lauke, and Y. W. Mai, "Effects of particle size, particle/matrix interface adhesion and particle loading on mechanical properties of particulate-polymer composites," *Compos. Part B Eng.*, vol. 39, no. 6, pp. 933–961, 2008, doi: 10.1016/j.compositesb.2008.01.002.
- [7] X. Zhao, Q. Zhang, and D. Chen, "Enhanced Mechanical Properties of Graphene-Based Poly(vinyl alcohol) Composites," *Macromolecules*, vol. 43, no. 5, pp. 2357–2363, 2010, doi: 10.1021/ma902862u.
- [8] J. Shang *et al.*, "Effect of folded and crumpled morphologies of graphene oxide platelets on the mechanical performances of polymer nanocomposites," *Polymer (Guildf)*, vol. 68, pp. 131–139, 2015, doi: 10.1016/j.polymer.2015.05.003.
- [9] T. D. Thanh, L. Kaprálková, J. Hromádková, and I. Kelnar, "Effect of graphite nanoplatelets on the structure and properties of PA6-elastomer nanocomposites," *Eur. Polym. J.*, vol. 50, no. 1, pp. 39–45, 2014, doi: 10.1016/j.eurpolymj.2013.10.022.
- [10] C. Wan and B. Chen, "Reinforcement and interphase of polymer/graphene oxide nanocomposites," *J. Mater. Chem.*, vol. 22, no. 8, pp. 3637–3646, 2012, doi: 10.1039/c2jm15062j.
- [11] J. Qiu and S. Wang, "Enhancing Polymer Performance Through Graphene Sheets," *J. Appl. Polym. Sci.*, vol. 119, no. 6, pp. 3670–3674, 2011, doi: 10.1002/app.
- [12] B. Li and W. H. Zhong, "Review on polymer/graphite nanoplatelet nanocomposites," *J. Mater. Sci.*, vol. 46, no. 17, pp. 5595–5614, 2011, doi: 10.1007/s10853-011-5572-y.
- [13] J. Jin, R. Rafiq, Y. Q. Gill, and M. Song, "Preparation and characterization of high performance of graphene/nylon nanocomposites," *Eur. Polym. J.*, vol. 49, no. 9, pp. 2617–2626, 2013, doi: 10.1016/j.eurpolymj.2013.06.004.
- [14] X. Wang and M. Song, "Toughening of polymers by graphene," *Nanomater. Energy*, vol. 2, no. 5, pp. 265–278, 2013, doi: 10.1680/nme.13.00024.
- [15] D. Yuan, B. Wang, L. Wang, Y. Wang, and Z. Zhou, "Unusual toughening effect of graphene oxide on the graphene oxide / nylon 11 composites prepared by in situ melt polycondensation," *Compos. Part B*, vol. 55, pp. 215–220, 2013, doi: 10.1016/j.compositesb.2013.05.055.
- [16] A. O'Neill, D. Bakirtzis, and D. Dixon, "Polyamide 6/Graphene composites: The effect of in situ polymerisation on the structure and properties of graphene oxide and reduced graphene oxide," *Eur. Polym. J.*, vol. 59, pp. 353–362, 2014, doi: 10.1016/j.eurpolymj.2014.07.038.
- [17] K. P. Pramoda, H. Hussain, H. M. Koh, H. R. Tan, and C. B. He, "Covalent bonded polymer-graphene nanocomposites," *J. Polym. Sci. Part A Polym. Chem.*, vol. 48, no. 19, pp. 4262–4267, 2010, doi: 10.1002/pola.24212.
- [18] Z. Chen and H. Lu, "Constructing sacrificial bonds and hidden lengths for ductile graphene/polyurethane elastomers with improved strength and toughness," *J. Mater. Chem.*, vol. 22, no. 25, pp. 12479–12490, 2012, doi: 10.1039/c2jm30517h.

- [19] J. Wang *et al.*, “Synthesis , mechanical , and barrier properties of LDPE / graphene nanocomposites using vinyl triethoxysilane as a coupling agent,” *J Nanopart Res*, vol. 13, no. 2, pp. 869–878, 2011, doi: 10.1007/s11051-010-0088-y.
- [20] R. K. Layek, S. Samanta, and A. K. Nandi, “The physical properties of sulfonated graphene / poly ( vinyl alcohol ) composites,” *Carbon N. Y.*, vol. 50, no. 3, pp. 815–827, 2011, doi: 10.1016/j.carbon.2011.09.039.
- [21] L. Tang *et al.*, “The effect of graphene dispersion on the mechanical properties of graphene / epoxy composites,” *Carbon N. Y.*, vol. 60, pp. 16–27, 2013, doi: 10.1016/j.carbon.2013.03.050.
- [22] M. A. Rafiee *et al.*, “Fracture and Fatigue in Graphene Nanocomposites,” *Small*, vol. 6, no. 2, pp. 179–183, 2010, doi: 10.1002/sml.200901480.
- [23] M. Fang, Z. Zhang, J. Li, H. Zhang, H. Lu, and Y. Yang, “Constructing hierarchically structured interphases for strong and tough epoxy nanocomposites by amine-rich graphene surfaces,” *J. Mater. Chem.*, vol. 20, pp. 9635–9643, 2010, doi: 10.1039/c0jm01620a.
- [24] I. Kelnar *et al.*, “Effect of Graphene Oxide on Structure and Properties of Impact-Modified Polyamide 6,” *Polym. Plast. Technol. Eng.*, vol. 57, no. 9, pp. 827–835, 2018, doi: 10.1080/03602559.2017.1354223.
- [25] M. U. Wahit, A. Hassan, Z. A. M. Ishak, and T. Czigány, “Ethylene-octene copolymer (POE) toughened polyamide 6/polypropylene nanocomposites : Effect of POE maleation,” *Express Polym. Lett.*, vol. 3, no. 5, pp. 309–319, 2009, doi: 10.3144/expresspolymlett.2009.39.
- [26] S. Lim, A. Dasari, G. Wang, Z. Yu, Y. Mai, and Q. Yuan, “Impact fracture behaviour of nylon 6-based ternary nanocomposites,” *Compos. Part B*, vol. 41, no. 1, pp. 67–75, 2010, doi: 10.1016/j.compositesb.2009.03.006.
- [27] G. M. Shashidhara, D. Biswas, B. Shubhalaksmi Pai, A. K. Kadiyala, G. S. Wasim Feroze, and M. Ganesh, “Effect of PP-g-MAH compatibilizer content in polypropylene/nylon-6 blends,” *Polym. Bull.*, vol. 63, no. 1, pp. 147–157, 2009, doi: 10.1007/s00289-009-0074-7.
- [28] O. Norhayani, H. Azman, R. A. Razak, and W. M. Uzir, “Effects Of POE and POE-G-MA on impact and tensile properties of polyamide nanocomposites,” in *Simposium Polimer Kebangsaan Ke-V*, 2005, no. May 2014.
- [29] J. J. Huang, H. Keskkula, and D. R. Paul, “Comparison of the toughening behavior of nylon 6 versus an amorphous polyamide using various maleated elastomers,” *Polymer (Guildf.)*, vol. 47, no. 2, pp. 639–651, 2006, doi: 10.1016/j.polymer.2005.11.088.
- [30] S. M. Lai, Y. C. Liao, and T. W. Chen, “Properties and preparation of compatibilized nylon 6 nanocomposites/ABS blends using functionalized metallocene polyolefin elastomer. I. Impact properties,” *J. Appl. Polym. Sci.*, vol. 100, no. 2, pp. 1364–1371, 2006, doi: 10.1002/app.23630.
- [31] W. S. Chow, Z. A. M. Ishak, J. Karger-kocsis, A. A. Apostolov, and U. S. Ishiaku, “Compatibilizing effect of maleated polypropylene on the mechanical properties and morphology of injection molded polyamide 6/polypropylene/organoclay nanocomposites,” *Polymer (Guildf.)*, vol. 44, no. 24, pp. 7427–7440, 2003, doi: 10.1016/j.polymer.2003.09.006.
- [32] X. Fu, C. Yao, and G. Yang, “Recent advances in graphene/polyamide 6 composites: A review,” *RSC Adv.*, vol. 5, no. 76, pp. 61688–61702, 2015, doi: 10.1039/c5ra09312k.
- [33] D. Vroom, “Thermal and mechanical analysis of nylon 6 and nylon 6 , 6 blends,” 1997.
- [34] Y. Yang, M. Zhao, Z. Xia, H. Duan, G. Zhao, and Y. Liu, “Facile Preparation of Polyamide 6 / Exfoliated Graphite Nanoplate Composites via Ultrasound-Assisted Processing,” *Polym. Eng. Sci.*, vol. 58, no. 10, pp. 1739–1745, 2018, doi: 10.1002/pen.24773.
- [35] T. K. Das and S. Prusty, “Graphene-Based polymer composites and their applications,” *Polym. - Plast. Technol. Eng.*, vol. 52, no. 4, pp. 319–331, 2013, doi: 10.1080/03602559.2012.751410.